JGR Biogeosciences

RESEARCH ARTICLE
10.1029/2020JG005693

Key Points:
- A growing lens of freshwater in the Arctic Ocean continues to expand after the year 2100 in CESM1(BGC) for RCP 8.5
- The expanding freshwater lens increases nutrient stress, overriding gains in marine productivity associated with sea ice loss
- By 2300, export production declines by 53% and the peak bloom shifts from July to May, strongly influencing arctic marine food web dynamics

Supporting Information:
- Supporting Information S1

Correspondence to:
W. Fu,
weiweif@uci.edu

Citation:
Fu, W., Moore, J. K., Primeau, F. W., Lindsay, K., & Randerson, J. T. (2020). A growing freshwater lens in the Arctic Ocean with sustained climate warming disrupts marine ecosystem function. *Journal of Geophysical Research: Biogeosciences*, *125*, e2020JG005693. https://doi.org/10.1029/2020JG005693

Received 13 FEB 2020
Accepted 18 NOV 2020
Accepted article online 4 DEC 2020

A Growing Freshwater Lens in the Arctic Ocean With Sustained Climate Warming Disrupts Marine Ecosystem Function

Weiwei Fu[1], J. Keith Moore[1], François W. Primeau[1], Keith Lindsay[2], and James T. Randerson[1]

[1]Department of Earth System Science, University of California, Irvine, CA, USA, [2]Climate and Global Dynamics Division, National Center for Atmospheric Research (NCAR), Boulder, CO, USA

Abstract One of the most robust changes in the hydrological cycle predicted by Earth System Models (ESMs) during the remainder of 21st century is an increase in the difference between precipitation and evapotranspiration (P-E) in arctic and boreal regions. We explore the long-term consequences of this change for marine ecosystems in the Arctic Ocean using the Community Earth System Model forced with a business as usual scenario of future greenhouse gas concentrations. We find that by the year 2300 increases in freshwater delivery considerably reduce Arctic Ocean surface salinity, creating a freshwater lens that has far-reaching impacts on marine biogeochemistry. The expanding freshwater lens limits vertical nutrient supply into the euphotic zone by enhancing vertical stratification and accelerating surface lateral mixing with surface waters in the North Atlantic, which become increasingly nutrient depleted from weakening of the Atlantic Meridional Overturning Circulation (AMOC). The resulting increase in nutrient stress reduces marine export production in the Arctic Ocean by 53% in 2300 relative to the 1990s and triggers a shift in community composition with small phytoplankton replacing diatoms. At the same time, the seasonal timing of export production undergoes a 2-month forward shift, with the peak advancing from July to May. This suggests that the threat to food webs and higher trophic levels may intensify after the year 2100 as gains in productivity from sea ice loss saturate and freshwater impacts on nutrient stress continue to strengthen. Our analysis highlights the critical importance of changing terrestrial hydrology and land-ocean coupling as drivers of long-term biogeochemical change in the Arctic Ocean and the necessity of multi-century climate change projections.

Plain Language Summary Climate warming will cause more rain and snow to fall in northern regions, increasing river runoff and causing the Arctic Ocean to freshen. Using a global climate model, here we explore the long-term consequences of this freshening for the marine biosphere. As the Earth responds to a future scenario of “business-as-usual” fossil fuel emissions, an expanding lens of freshwater will form a cap on the surface of the Arctic Ocean, limiting the upward mixing of nutrient-rich water from deeper ocean layers. This stunts the growth of phytoplankton, counteracting by 2100 gains in marine productivity caused by increasing light availability from sea ice loss. After 2100, as the freshwater cap strengthens, small phytoplankton mostly replace diatoms in arctic ecosystems as a consequence of increasing nutrient stress. This transition happens rather suddenly, suggesting that the marine biosphere may pass through an ecological tipping point. By 2300, export production, a measure of the flow of organic matter available to support zooplankton, fish, and marine mammals, declines by over 50%. At the same time, a shift in the timing of the peak phytoplankton bloom from July to May is likely to further disrupt arctic food webs. Our work shows that climate change impacts on the hydrological cycle in the far north will have long-lasting and far-reaching impacts on the marine biosphere in the Arctic and highlights the importance exploring the potential for ecological tipping points in deep future time.

1. Introduction

Since the 1970s, the Arctic Ocean has experienced unprecedented increases in freshwater inputs from river runoff, precipitation, and melting glaciers that have been attributed to climate warming (Haine et al., 2015; McPhee et al., 2009; Peterson et al., 2002). The increases in freshwater, if sustained, are likely to have a myriad of impacts on sea ice, basin and global-scale ocean circulation, and marine biogeochemistry

(Carmack et al., 2016). Increases in freshwater enhance stratification and reduce mixed layer depths within the Arctic (Pemberton & Nilsson, 2016), which in turn constrains the upward diffusive flux of heat from warmer subsurface Atlantic and Pacific Ocean inflows (Carmack et al., 2016; Nummelin et al., 2016; Polyakov et al., 2013). Simulations with climate models suggest that increasing precipitation in the Arctic may act as a negative feedback to climate warming by slowing the loss of sea ice (Bintanja et al., 2018; Carmack et al., 2015; Nummelin et al., 2016). Freshwater export from the Arctic also strongly influences deep water formation in the North Atlantic and Labrador Sea and potentially influences the intensity of Atlantic Meridional Overturning Circulation (AMOC) (Koenigk et al., 2007; Rennermalm et al., 2006; Yang et al., 2016), which is of great importance for ocean heat transport and global climate (Dong et al., 2009; Drijfhout, 2015; Oldenburg et al., 2018). With further climate warming, freshwater inputs to the Arctic Ocean are projected to strongly increase during the latter half of the 21st century (Collins et al., 2013; Shu et al., 2018).

Sustained long-term increases in freshwater have the potential to affect a broad suite of productivity and ecological responses in the Arctic Ocean (Carmack et al., 2016; Carmack & McLaughlin, 2011; Coupel et al., 2015; Li et al., 2009). Nutrient supply to the surface is suppressed when freshwater inputs weaken vertical mixing that normally brings up nutrients from deeper layers (Carmack et al., 2016; Carmack & McLaughlin, 2011; Pemberton & Nilsson, 2016; Tremblay et al., 2015; Williams & Carmack, 2015). Both freshwater increases and retreating sea ice are important factors regulating contemporary marine net primary production (NPP) in the Arctic, yet the interplay between these drivers is complex and likely varies by region. Over the past several decades, increases in Arctic Ocean NPP have been attributed primarily to loss of sea ice cover, which boosts light availability, prolongs the growing season, and allows for increases in wind-driven vertical mixing in open water (Arrigo & van Dijken, 2011, 2015; Vancoppenolle et al., 2013). In coastal-shelf environments, freshening of surface waters may have damped these trends (Coupel et al., 2015), particularly during the latter part of the growing season where satellite observations provide evidence for strengthening fall phytoplankton blooms (Ardyna et al., 2014). In Earth System Model (ESM) simulations to the year 2100, most but not all models predict increasing Arctic Ocean productivity as a consequence of continued sea ice cover declines, although nutrient limitation is expected to intensify (Moore et al., 2013; Vancoppenolle et al., 2013).

Beyond 2100, however, interactions between changing sea ice and freshwater inputs are not well understood and have not been systematically explored using fully coupled ESMs. For moderate and high fossil fuel emissions scenarios, the relative importance of sea ice and freshwater drivers may be expected to change, as these processes respond on different time scales to external forcing from the global Earth System. Near complete loss of sea ice cover during spring, summer, and fall is expected during 22nd century for the representative concentration pathway 8.5 (RCP 8.5) (Hezel et al., 2014). The impacts of changing sea ice cover on light availability will saturate as the sea ice disappears. In contrast, the impacts of increasing freshwater inputs on surface salinity and stratification in the Arctic Ocean may evolve over a different timescale that is determined in part by river runoff and the degree to which lateral mixing with surface waters in Atlantic and Pacific Ocean basins allows surface salinity in the Arctic to reach a new steady state. Developing a mechanistic understanding of likely changes in Arctic Ocean productivity on these longer timescales is critical for understanding how 21st century decisions regarding fossil fuel use will ultimately affect arctic biogeochemical cycling, ecosystem functioning, and ecosystem services over the next millennium.

Here we explore the contrasting biogeochemical impacts of changing sea ice cover and freshwater inputs for marine ecosystems in the Arctic Ocean to the year 2300 using a fully coupled ESM. In our analysis we use the Community Earth System Model (CESM1[BGC]) which generally captures the observed spatial distribution of nutrients, surface salinity, and sea ice cover patterns for the present day (Moore et al., 2013). We believe that this exploration beyond 2100 is important for identifying new mechanisms and potential tipping points that may influence the long-term sustainability of arctic ecosystems. In this context, mechanisms we uncover may help inform science priorities for future field and modeling initiatives and provide greater motivation for meeting emissions reductions. We previously examined the evolution of the climate-carbon feedbacks and warming trends (Randerson et al., 2015) and interactions between land use change and carbon cycle feedbacks from this simulation (Mahowald et al., 2017). We also documented a climate-driven

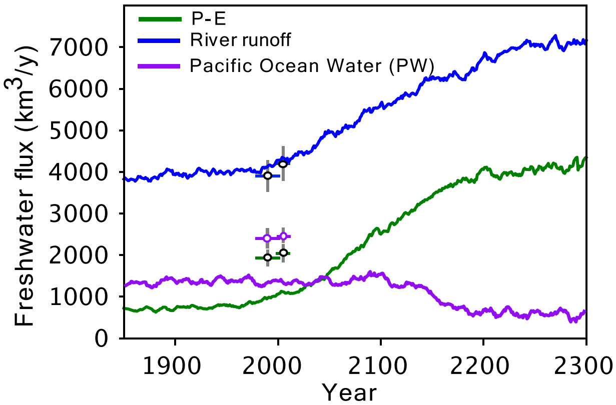

Figure 1. Freshwater flux from river runoff, precipitation minus evaporation (P-E), and Pacific Ocean water (PW) in the Arctic Ocean (70–90°N). Model estimates are shown with solid lines from CESM1(BGC) for the RCP 8.5 scenario. Observations for P-E over the ocean surface north of 70°N were derived from the ERA-INTERIM atmospheric reanalysis product (Dee et al., 2011). Pan-Arctic runoff estimates (open circles) for the period of 1980–2000 and 2000–2010 are shown from Haine et al. (2015), which were derived from the ERA-INTERIM atmospheric reanalysis product and river discharge observations extrapolated to fill substantial data gaps. Observations of freshwater inflow from the Pacific Ocean through Bering Strait are also taken from Haine et al. (2015). Horizontal bars with open circles denote the observations for the period of 1980–2000 and 2000–2010, respectively. Vertical bars on the circles indicate the uncertainty range of the observations.

sequestration of nutrients in the deep ocean, driven by changing circulation and strong nutrient trapping in the Southern Ocean (Moore et al., 2018).

Our simulation shows that by 2100 NPP in the Arctic Ocean increases as a consequence of climate warming, in a manner consistent with other CMIP5 models, as declining sea ice cover increases light availability and the length of the ice-free growing season. In past work, Slagstad et al. (2015) found that changing sea ice and stratification together influence levels of primary production in different regions of the Arctic Ocean for the International Panel of Climate Change (IPCC) A1B climate scenario. More recently, Randelhoff et al. (2020) found that turbulent vertical nitrate fluxes play a critical role in regulating primary production in the Arctic Ocean. Here we show that multi-century increases in freshwater inputs significantly reduce surface salinity, causing increasing stratification and widespread changes in marine ecosystem dynamics. The growing freshwater lens overrides other controls on productivity after 2100, highlighting the potential for far-reaching impacts on food webs and biodiversity in the Arctic.

2. Results

2.1. Freshwater Runoff in the Arctic Ocean

With climate warming, freshwater fluxes to the Arctic Ocean increase substantially from changes in river runoff and the difference between precipitation and evapotranspiration (P-E) over the ocean surface (Figure 1). River runoff is the largest source of freshwater to the Arctic Ocean, and this flux gradually increases from 3,900 km^3/year during 1850s to 7,100 km^3/year during the 2290s. During the contemporary era, CESM1(BGC) predicts that river runoff increases from 4,010 km^3/year during 1980–2000 to 4,130 km^3/year during 2000–2010. These changes are comparable to the observed trends for these time intervals reported by Haine et al. (2015), with estimates of 3,900 ± 390 km^3/year during 1980–2000 and 4,200 ± 420 km^3/year during 2000–2010.

Concurrently, P-E over the Arctic Ocean increases by about fivefold in CESM1(BGC) over the course of this simulation, from 730 km^3/year in the 1850s to 4,150 km^3/year during the 2290s. Model estimates of P-E for the contemporary era are somewhat lower than estimates derived from reanalysis (Figure 1) but show similar trends (Haine et al., 2015). P-E accounts for 14% of freshwater input in the 1990s, but this fraction increases over time in the future as P-E over the open ocean increases more rapidly than runoff. Pacific Ocean water (PW) is another important source of freshwater for the Arctic Ocean. In CESM1(BGC), the input of freshwater from PW remains relatively stable to year 2100 and then declines (Figure 1). During the 1980–2000 period, CESM1(BGC) estimates the PW flux to be 1,360 km^3/year, which is lower than the estimate of 2,400 km^3/year through the Bering Strait reported by Haine et al. (2015). Altogether, Arctic Ocean freshening in CESM1(BGC) from the 1990s to the 2290s is driven primarily by increases in river and P-E fluxes; the concurrent declines in PW are much smaller in magnitude and only partly offset the larger gains from the other two terms.

2.2. Physical and Biogeochemical Impacts

Arctic Ocean salinity shows a clear response to the polar amplification of the hydrological cycle. By the 2290s, surface salinity decreases by 9.7% for the Arctic Ocean as a whole relative to the 1990s (Figure 2a) and by up to 34% in coastal seas such as the East Siberian Sea and Laptev Sea (Figure 3). The declines in salinity in the Arctic Ocean are the largest predicted for any ocean basin in CESM1(BGC) and are balanced by increases in salinity in the tropical and southern Atlantic Ocean and in the Indian Ocean (Figure S1 in the supporting information). In the Greenland Sea, an important path for surface waters flowing from the Arctic Ocean into the North Atlantic, salinity decreases by 11% in the 2290s relative to the 1990s. Ocean salinity observations show a "rich get richer" mechanism in the global ocean with fresh regions becoming fresher

10.1029/2020JG005693

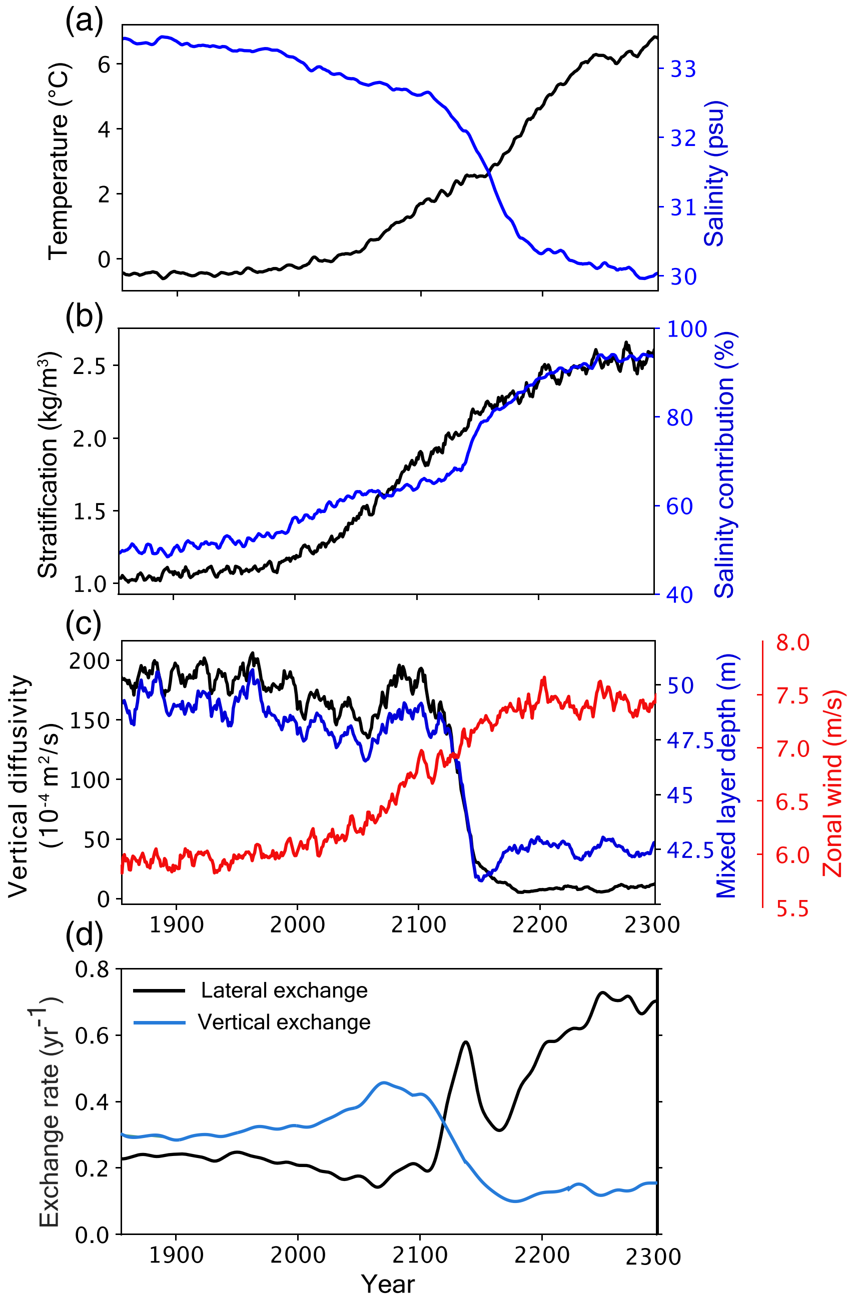

Figure 2. Time series of physical changes of the Arctic Ocean from CESM1(BGC) for the RCP 8.5 scenario. (a) Mean temperature and salinity for a depth of 0–150 m for the Arctic Ocean north of 70°N; (b) a stratification index (kg/m^3) derived from density differences between the surface and 150 m along with the contribution of salinity to this index; (c) total vertical diffusivity, mean mixed layer depth, and surface zonal wind speed; and (d) water exchange rate between the surface ocean (0–150 m) and the subarctic North Atlantic (lateral exchange) and the subsurface Arctic Ocean below 150 m (vertical exchange).

and salty regions becoming saltier in response to observed warming (Durack et al., 2012). CESM1(BGC) shows the same pattern intensifying over time. The mean sea surface salinity (SSS) gradient between the tropical Atlantic and North Atlantic Ocean increases and is consistent with expectations of greater evaporation in the northern tropical Atlantic and much stronger poleward transport of water vapor within the atmosphere in response to climate warming. By 2300, surface salinity in the Arctic has not established a new steady state and is continuing to decline.

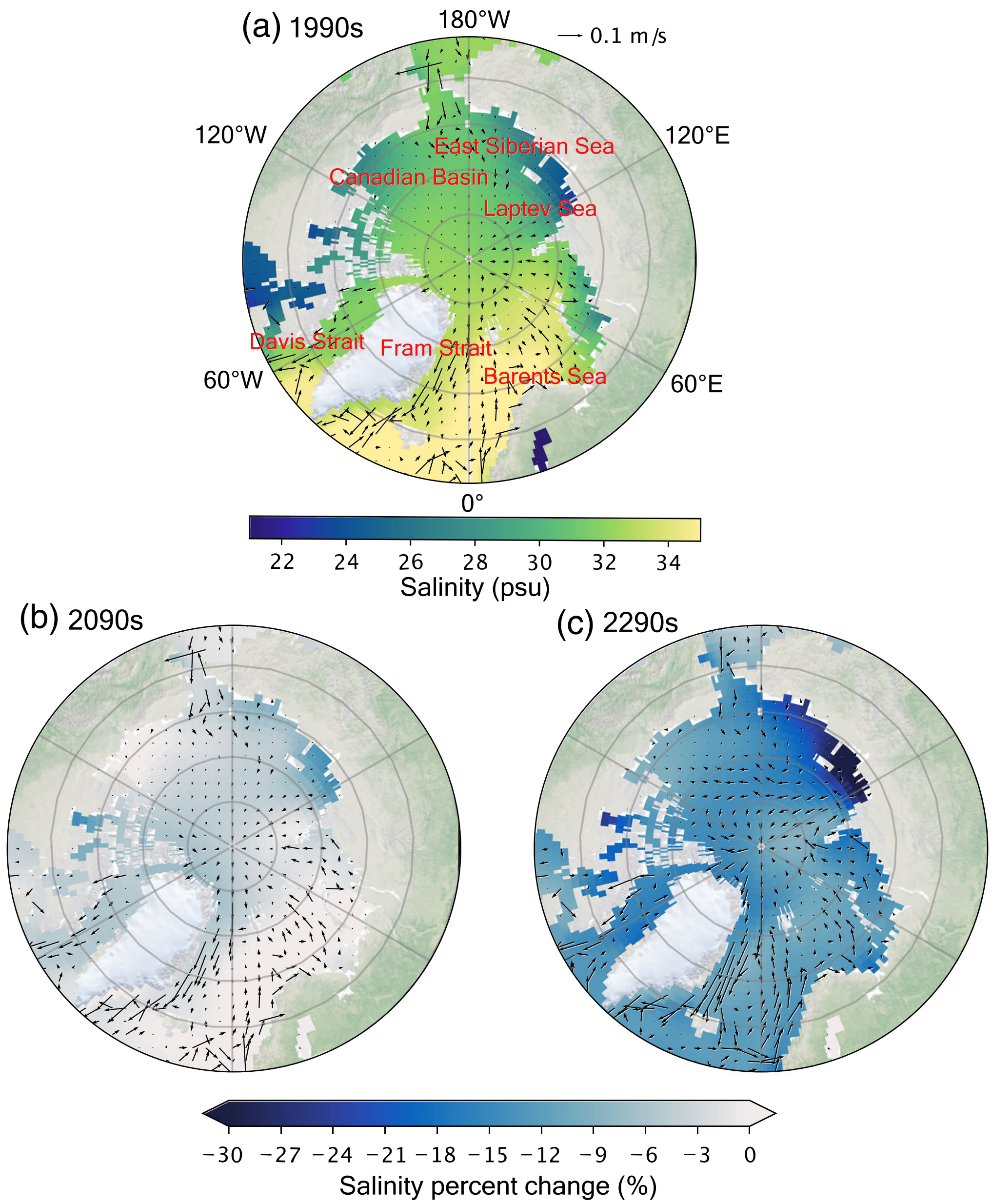

Figure 3. Changes in Arctic Ocean salinity and surface currents. (a) Sea surface salinity (SSS) during the 1990s and percent change of SSS relative to 1990s for (b) the 2090s and (c) the 2290s from the CESM1(BGC) model for RCP 8.5. The overlying vectors indicate ocean surface currents for the 1990s, 2090s, and 2290s, respectively.

The strength of ocean surface currents into and out of the Arctic Ocean intensify in parallel with changes in salinity and sea ice cover. More freshwater is exported out of the Arctic Ocean as surface currents become stronger in Fram and Davis Straits. By the 2290s, the freshwater flux out of the Arctic Ocean by means of the Fram Strait increases from 1,950 km^3/year to 5,890 km^3/year relative to the 1990s. The estimate is based on a reference salinity of 34.80 (Haine et al., 2015). For the Davis Strait, the freshwater flux increases from 2,300 km^3/year to 4,300 km^3/year (Figure S2). Both the salinity and velocity anomalies play a role in the variation of the freshwater export (Jahn et al., 2012). The flux estimates for these two Straits predicted by our model are lower than estimates reported by Haine et al. (2015) and Carmack et al. (2016) for the periods of 1980–2000 and 2001–2010, respectively. The surface salinity changes (Figure 3) indicate that a significant fraction of the exported freshwater ultimately reaches the Labrador Sea (Yang, Dixon, et al., 2016) and thus has the potential to modify North Atlantic deep water formation.

Arctic Ocean surface water concurrently warms, with temperatures increasing by 6.5°C in the upper 150 m from the 1990s through the 2290s (Figure 2a). Together, both warming and freshening contribute to stratification increases in the Arctic Ocean. A stratification index, defined as the difference in density between 150 m and the surface, increases from about 1.1 kg/m^3 in the 1990s to 2.5 kg/m^3 by the 2290s (Figure 2b). Salinity becomes increasingly important as the driver of stratification, accounting for about 93% of the density gradient by the 2290s. The strong vertical salinity gradient in the Arctic today gets much stronger with climate warming. Enhanced stratification results in shallower mixed layer depths and smaller vertical diffusivities (Figure 2c), both of which show rapid declines between 2100 and 2150. Mixed layer depth in the Arctic Ocean declines from a mean of about 48 m during the 1990s to about 43 m by the 2290s as sea ice disappears.

Recent work emphasizes winds as an important driver of northern high-latitude ocean overturning (Yang et al., 2016). We find that in CESM zonal westerly winds between 70°N and 90°N increase by about 30% between 2000 and 2200 and then level off (Figure 2c), following a trajectory that is closely (and negatively) related to the decline in sea ice. Zonal mean wind increases are known to be associated with the loss of sea ice, which decreases surface roughness and lower-tropospheric stability (Mioduszewski et al., 2018). Despite the increasing wind stress within CESM, stratification induced by the increasing freshwater inputs more than compensates for the stronger winds (Figure 2b).

A box model derived from different physical and biogeochemical tracers from the full CESM1(BGC) simulation (Fu et al. (2018); see section 4) revealed that lateral water exchange between the Arctic and subarctic North Atlantic also increases over time (Figure 2d), in a manner consistent with the increasing velocity of surface currents (Figure 3). The box model also shows a decline in vertical exchange, which is consistent with the decreasing vertical diffusivity obtained from the full model.

Nitrate concentration in the upper 150 m of the Arctic Ocean declines nearly threefold by the 2290s, with the most rapid change occurring between 2050 and 2150 (Figure 4). The nutrient decline is a consequence of two separate and reinforcing mechanisms. First, the nutrient supply from deep water is inhibited due to stratification increases that reduce vertical mixing (Figures 2d and S3). Second, the accelerating lateral exchange with surface waters of the North Atlantic Ocean further reduces surface nutrients because upper ocean North Atlantic waters become increasingly nutrient depleted as a consequence of AMOC slowdown and reductions in deep mixing during winter (Figure S3; Moore et al., 2013). Nutrient trapping in the Southern Ocean also reduces the northward flux of nutrients into the Atlantic basin after 2100 (Moore et al., 2018). Only two other CMIP5 models conducted long-term simulations to the year 2300 (MPI-ESM-LR, Giorgetta et al., 2013, and HadGEM2-ES, Caesar et al., 2013) and submitted output to the Earth System Grid Federation. Both models show long-term increases in freshwater inputs from P-E and river runoff and concurrent declines in surface NO_3 concentrations in Arctic Ocean surface waters (Figure S4), providing evidence for a biogeochemical response to intensification of the northern hydrological cycle that is robust across different model formulations.

2.3. Marine Ecosystem Response

Arctic Ocean productivity is co-limited by light and nutrients (Popova et al., 2012), with the importance of these factors varying over time in our simulation. By the 2090s the annual particulate organic carbon (POC) flux decreases in CESM1(BGC) by a relatively modest amount (7%) (Figure 4b), with increases of photosynthetically available radiation (PAR) from loss of sea ice nearly balancing decreases caused by declining nutrient availability (Figure 4d). The annual cycle, however, is considerably modified as loss of sea ice enhances the productivity in the spring. Increasing export of organic matter during the spring bloom, in turn, strips out nutrients from surface waters and subsequently intensifies nutrient limitation (and productivity losses) during summer and fall (Figure 4c). By the 2150s there is no summer sea ice and by the 2200 s there is no winter sea ice (Figure S5). As a result, productivity gains from changing light availability level off after 2150, but nutrient stress continues to grow as stratification increases from increasing fresh water inputs and changes in the circulation and biogeochemistry of the North Atlantic. By the 2290s, the annual POC flux in the Arctic Ocean is greatly reduced by the long-term declines in nutrient availability, declining 53% relative to the 1990s (Figure 4b).

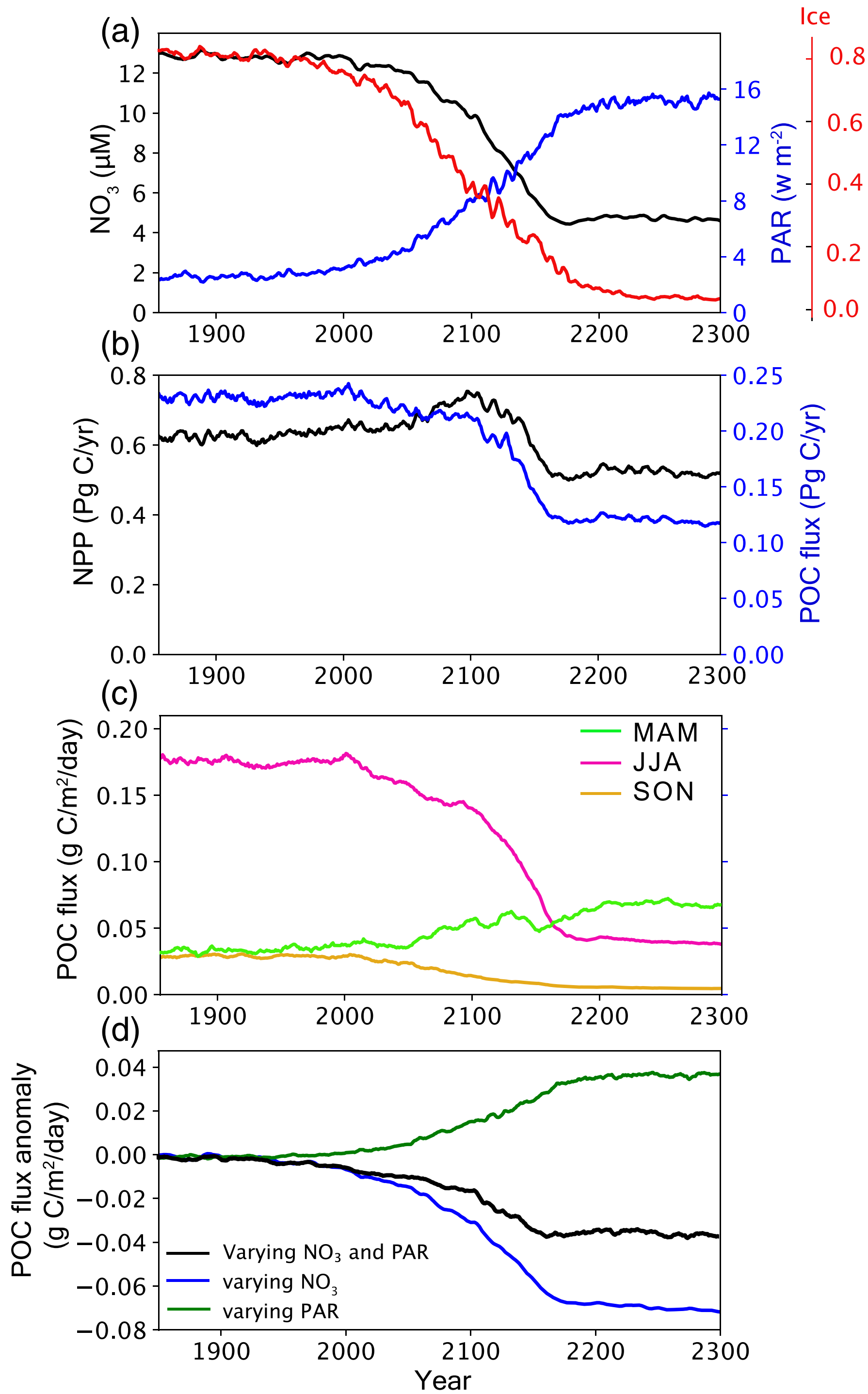

Figure 4. Time series of biogeochemical changes of the Arctic Ocean from CESM1(BGC) for the RCP 8.5 scenario. (a) Mean annual surface PAR and NO_3 for a depth of 0–150 m, along with annual mean sea ice fraction; (b) net primary production (NPP) and export production (POC flux) at a depth of 100 m; (c) POC fluxes during March–May, June–August, and September–November seasonal periods; and (d) the evolving contribution of light and nutrient to the change of POC flux derived from a regression model fit to monthly PAR and nitrate time series in 1990 from the full CESM1(BGC) simulation.

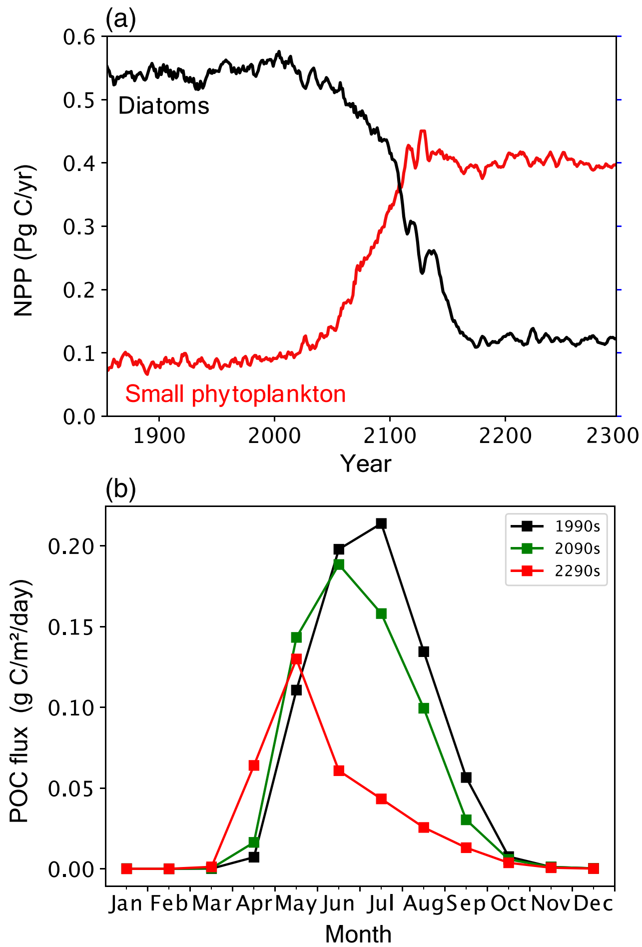

Figure 5. Changes in the composition and timing of marine net primary production and export production. (a) Time series of NPP from diatoms and small phytoplankton during the period of 1850–2300 and (b) seasonal changes of export production (POC flux at 100 m) for the 1990s, 2090s, and 2290 s from CESM1(BGC) for the RCP 8.5 scenario in the Arctic Ocean north of 70°N.

To separate the contribution of light and nutrients to the time-evolving POC flux at 100 m, we used a regression model with two driver variables that we identified as being critical for regulating the spatial and temporal dynamics of export production. The two variables were mean PAR at the ocean surface (under any sea ice) and NO_3 averaged over a depth range of 0–100 m from CESM1(BGC). The regression model captures the spatial-temporal distribution of the monthly mean POC flux during the 1990s (Figures S6a–S6c) with a correlation coefficient of 0.81. In addition, it is able to predict the evolution of POC flux over the period of 1850–2300 (Figure S6d). To identify the relative importance of PAR and NO_3, we held one variable fixed at levels in the 1850s and let the other evolve with time. The impact of varying PAR or nitrate shows that the role of nutrients dominates the trend in the POC flux after 2050. Specifically, this analysis revealed the strong opposing impacts of PAR and NO_3 on the evolution of the POC flux within the Arctic Ocean. Potential reductions in the POC flux from nutrient stress are about twice the magnitude of potential gains from increasing light availability between 2100 and 2200, and as consequence the POC flux declines sharply during this time (Figure 4d). The diagnosed impacts of light and nutrient on the POC flux level off after 2200 suggesting that arctic ecosystems may be approaching a new low-productivity steady state.

Increasing nutrient limitation also drives a shift in community composition. As a result of sustained long-term decreases in surface nitrate concentrations throughout the Arctic Ocean (Figure S3c), a rapid transition from a diatom-dominated system to a small phytoplankton-dominated system occurs between 2050 and 2150 (Figure 5a). This shift in community composition within the model is consistent with contemporary shipboard observations that show picoplankton increase in abundance and larger plankton decrease in abundance as nutrients and salinity decline in the Canadian Arctic (Li et al., 2009). After 2150, annual NPP stabilizes and is dominated by small phytoplankton.

With surface warming and sea ice retreat, the spring-summer bloom in the Arctic Ocean still remains the major annual primary production event for carbon export to higher trophic levels, but the timing of the peak bloom shifts 2 months earlier in the 2290s relative to 1990s (Figure 5b). The annual cycles of nitrate concentrations from 0–150 m vary less from century to century than the seasonality of NPP and POC flux (Figure S7), although the magnitude of the available inventory declines considerably. By 2300, the peak of PAR shifts earlier in the season, from July to June, and the increases in early season PAR are a primary driver of the POC flux increases during April and May. The earlier bloom increases nutrient stress in subsequent months, including for phosphate and iron (data not shown) in addition to nitrate. The increasing nutrient stress that emerges later in the growing season contributes to the community shift in phytoplankton composition shown in Figure 5a and counteracts the effect of a prolonged growing season on annual NPP. The community shift decouples POC flux from NPP (increasing the fraction of NPP supported by regenerated nutrients) and likely reduces organic matter flows to higher trophic levels (Ceballos-Romero et al., 2016; Le Moigne et al., 2015; Moore et al., 2013).

In eight geographic regions of the Arctic Ocean (Arrigo & van Dijken, 2015), we find that the decrease in magnitude of the peak bloom and its phase are consistent across the different sectors, with about a 1 month forward shift predicted for the Barents and Greenland Seas and about a 2 month shift predicted for the other six sectors (Figure 6). In the different sectors, the seasonality change of POC flux depends on how increasing PAR interacts with declining nutrient availability. The phase shift is weaker in the Greenland and Barents Sea because there is less ice cover initially and higher nutrient availability. The forward shift in the bloom

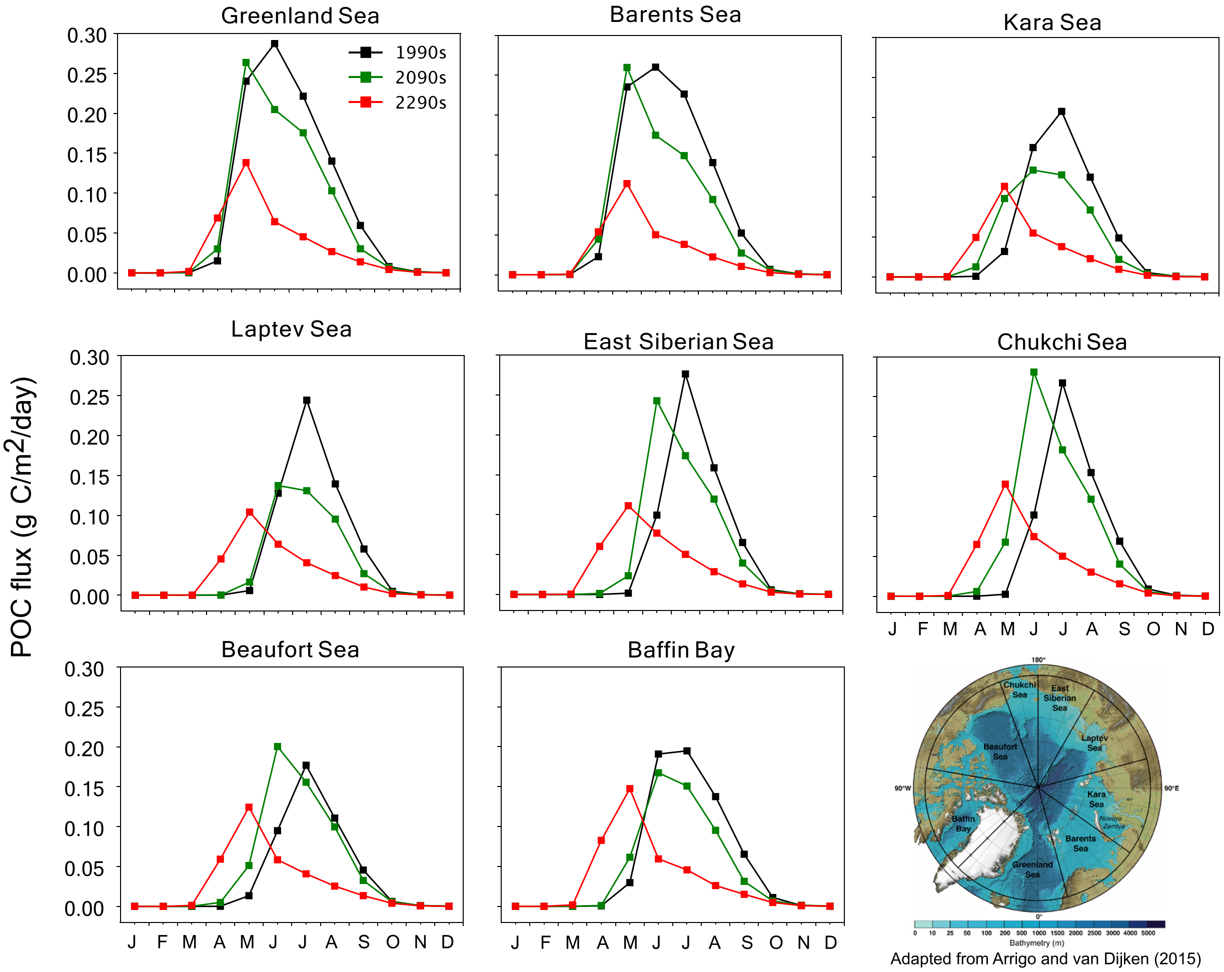

Figure 6. Change in the annual cycle of POC flux in eight sectors of the Arctic Ocean for the 1990s, 2090s, and 2290s. The sectors used here followed the definition by Arrigo and van Dijken (2015). The POC flux (export production) from CESM1(BGC) for the RCP 8.5 scenario is shown at a depth of 100 m.

predicted here for open ocean phytoplankton appears to be largely synchronized with phenology model predictions for sea ice algae (Tedesco et al., 2019), potentially amplifying risks to food sources for higher trophic levels during late summer.

The phytoplankton community shift decouples export production from NPP and reduces organic matter flows to higher trophic levels (Ceballos-Romero et al., 2016; Le Moigne et al., 2015; Moore et al., 2013). The shift to small phytoplankton results in less efficient export of organic matter and enhanced recycling of nutrients within surface waters, driving increases in regenerated primary production. This explains why export production declines much more than NPP (Figure 5). The increase in regenerated primary production, however, fueled by surface recycling of nutrients, does not provide additional food for higher trophic levels. Thus, we suggest that changes in export production, which are closely correlated with new production (and fueled by new nutrient inputs), are a better metric for climate impacts on food webs than changes in NPP.

3. Discussion and Conclusions

The Arctic Ocean is the most riverine-influenced of the world's major oceans, and the importance of terrestrial nutrients in this environment is poorly understood (Tank et al., 2012; Torres-Valdés et al., 2013). In CESM1(BGC), as is the case for almost all CMIP-class ESMs, land and ocean nutrient cycles are independent and decoupled. An important next step in this context is to strengthen the representation of terrestrial nutrient flows (including dissolved organic nutrients, mineralization and nitrification), subsequent loading of nutrients in rivers, and ultimately transport through river, estuarine, and coastal ecosystems to the open ocean. Le Fouest et al. (2013) found that the contribution of riverine nitrate to new primary production is small at the regional scale and negligible at the pan-Arctic scale with historical data (1954–2012). We hypothesize, however, that with an expanding freshwater lens in the Arctic Ocean that reduces nutrient inputs from below, the importance of the riverine nutrients will grow stronger, particularly in regions of the largest surface salinity declines. As a result, Arctic Ocean nutrient availability may become increasingly dependent on rates of permafrost melt (Kipp et al., 2018), wildfires (Veraverbeke et al., 2017), soil drainage (Reyes & Lougheed, 2015), and other factors known to regulate nutrient losses from arctic and boreal terrestrial ecosystems. We also note that CESM1(BGC) and other CMIP models do not yet have fully interactive ice sheet models for Greenland or Antarctica. Ice sheet melting on Greenland would even further amplify freshwater inputs to the Arctic Ocean, intensifying the freshwater lens. Since meltwater from glaciers is nutrient depleted (Hopwood et al., 2020), additional freshwater inputs from Greenland would further reduce nutrient availability and NPP.

Increasing export of freshwater from surface layers of the Arctic Ocean may also have the potential to interact with and slow the AMOC (Keigwin et al., 2018). In CESM1(BGC), much of the accelerating freshwater export from the Arctic Ocean flows through the Davis Straight on the west side of Greenland and through the Fram Strait between the east side of Greenland and Svalbard as an intensification of the East Greenland Current (Figures 3 and S2). From a biogeochemical systems perspective, if these flows weaken overturning circulation in the Labrador Sea and other centers of deep convection, they have the potential to amplify nutrient stress and ecosystem impacts in the Arctic and across the high-latitude North Atlantic. The degree to which these interactions in the North Atlantic affect productivity in the Arctic Ocean is difficult to assess with our single fully coupled CESM1(BGC) simulation. In this context, an important next step is to conduct partially coupled model experiments, in which, for example, the ocean experiences changing freshwater inputs from a fully coupled simulation, but forcing from greenhouse gases, aerosols, and other anthropogenic drivers is held at pre-industrial levels.

Reducing uncertainties in these long-term biological predictions may be possible in future work by exploring the robustness of freshwater lens and its biogeochemical impacts using different ESMs and different scenarios of future change. In this context, a longer, multi-century view is necessary for understanding the cumulative effects of 21st century decisions regarding our use of fossil fuels. New field observations and additional, higher-resolution modeling work are also necessary to better understand trade-offs between increasing open ocean wind stress and freshwater-driven changes in stratification, as this balance will ultimately regulate the availability of nutrients in surface waters of the Arctic Ocean.

The amplification of the northern hydrological cycle creates a lens of freshwater in the Arctic Ocean that is likely to persist for centuries. Sustained increases in freshwater runoff strengthen vertical stratification in the upper ocean and accelerate water exchange with the North Atlantic, depleting upper ocean nutrients. This effect more than counterbalances productivity gains from sea ice loss and a longer growing season in the Arctic Ocean, resulting in strong declines in export production after 2100. While the increase in stratification monotonically evolves from 1850 to 2300 (Figure 2b), most of the loss of diatoms (and rise of small phytoplankton) occurs over a relatively brief 100 year interval between 2050 and 2150, highlighting the potential for the Arctic Ocean to cross a biogeochemical tipping point. Indeed, this biological transition appears to be one of the main drivers of the rapid decline in export production during the 22nd century. More work is needed to examine non-linearities in the biogeochemical response of the Arctic Ocean to freshwater inputs, through a combination of field experiments and high-resolution model simulations of deep future time.

In the CESM1(BGC) simulation we analyzed here, the freshwater lens is still growing at 2300, albeit at a lower rate. We were unable to identify other environmental drivers that can sufficiently overcome the inertia of this freshwater lens, and longer simulations are needed as an important next step. Thus, the transition of the arctic marine ecosystems to a nutrient-limited, oligotrophic productivity regime appears irreversible until the freshwater lens dissipates. This seems unlikely except as climate cools on millennial timescales and the massive changes in the arctic hydrological cycle are reversed.

Together, the more than 50% declines in export production, loss of diatom productivity, and changes in the phase of the annual cycle suggest longer and less efficient food chains and declining biomass at higher trophic levels in the Arctic Ocean for a future world that follows the RCP 8.5 scenario of fossil fuel emissions. Our results are particularly concerning for all the ice-dependent and ice-obligate organisms in the Arctic, as the disappearance of the sea ice cover will be accompanied by a drastic reduction in food supply. Thus, higher trophic levels will become increasingly vulnerable to the effects of climate change, with implications for marine ecosystem management and the potential for developing Arctic fisheries. At a global scale, our analysis provides a novel example of how climate change impacts on terrestrial hydrology and land-ocean coupling may generate far-reaching ecological and biogeochemical consequences in downstream ocean ecosystems on multi-century timescales.

4. Methods

4.1. CESM1(BGC)

We conducted a 450 year simulation with Version 1 of the CESM1(BGC) spanning the period from 1850 to 2300. The prescribed atmospheric CO_2 time series consisted of three fused segments corresponding to historical, RCP 8.5, and ECP 8.5 atmospheric mole fractions. CO_2 mole fractions increased from approximately 285 ppm in 1850 to 1,962 ppm by 2250 (Randerson et al., 2015; van Vuuren et al., 2011). All of the other anthropogenic atmospheric forcing agents in this scenario were also radiatively coupled. These forcing agents included CH_4, N_2O, chlorofluorocarbons (CFCs), O_3, aerosols, and aerosol deposition on snow (Hu et al., 2013). External iron inputs to the oceans from the atmosphere and sediments were held constant over time using a climatology on monthly fluxes (Misumi et al., 2014). The ocean circulation model is the POP2 model (Danabasoglu et al., 2012). The phytoplankton community is represented by three explicit phytoplankton groups (diatoms, diazotrophs, and smaller phytoplankton) that compete for light and nutrients and all experience grazing pressure by a single, parameterized zooplankton group (Moore et al., 2004). Within CESM1(BGC) small phytoplankton are more competitive in nutrient-poor water masses, whereas diatoms thrive in more nutrient-replete areas. This is consistent with the patterns observed globally, with picophytoplankton dominating the community in the low-nutrient, oligotrophic subtropical gyres and diatom production increasing at high latitudes and in coastal upwelling zones. In CESM1(BGC), PAR is a function of surface shortwave radiation, an absorption coefficient for water (m), and an absorption coefficient for chlorophyll (m). It is strongly modulated by ice and snow cover. The PAR reaching the sea surface is a function of clouds and other atmospheric properties that change over time in the simulation. However, these changes are small compared to the step change that occurs when sea ice cover disappears.

In the Arctic Ocean, the model can reasonably simulate the spatial pattern of observed surface salinity, nitrate inventory, and sea ice concentration (Figure S8). Compared with the WOA13 data, nitrate inventory is reproduced higher in the central Arctic Ocean. For surface salinity, CESM1(BGC) can capture low salinity in the eastern Siberian Sea and Laptav Sea where strong river runoff occurs and high salinity in the advection domains of Atlantic water. CESM1(BGC) reproduces higher annual mean ice fraction in the Arctic Ocean than the NOAA/NSIDC data (Peng et al., 2013). Compared with other CMIP5 models, CESM1 (BGC) can reasonably capture the distribution of NO_3 for a depth of 0–150 m in the observations (Figure S9). To further evaluate the model in the Arctic Ocean, we compared the seasonal cycle of surface chlorophyll from CESM1(BGG) and other CMIP5 models with MODIS-Aqua satellite observations for the period of 2003–2016. Although the models show widely varying skills in the Arctic Ocean, and there are high levels of uncertainty associated with the observations, CESM1(BGC) tracks the annual cycle of the observations reasonably well (Figure S10). Additional documentation, source code, and model output are available online (www2.cesm.ucar.edu). The Arctic Ocean freshwater budget and flux calculations we used followed the approach described in Aagaard and Carmack (1989) and rely on 34.8 psu as the reference salinity, which is roughly the mean salinity of the Arctic Ocean.

4.2. Box Model

We created a box model of the arctic surface ocean using parameters calibrated quantitatively using available output from the full CESM1(BGC). The box model has a similar form to the approach described by Fu et al. (2018) and uses time evolving exchange coefficients to represent water exchange rates between different water masses. The model consisted of four boxes (Figure S11). The center box was defined as the surface of the Arctic Ocean, spanning 70–90°N and a depth range of 0–150 m. Boxes 1 and 2 were defined as comprising water masses in the sub-arctic North Pacific (50–70°N) and North Atlantic (50–70°N). Boxes 1 and 2 were defined to span the first 150 m, similar to the center box representing the surface of the Arctic Ocean.

We assumed that the major lateral transport from high latitudes North Atlantic and North Pacific occurred by means of flow between these boxes. Box 3 was used to constrain vertical exchange from below, spanning a depth range of 150–500 m.

The box model reproduced the temporal evolution of different tracers from the CESM1(BGC) model in arctic surface waters (Figure S12) reasonably well and also allowed us to quantify total advective and diffusive transport into the central box. The box model fit to the CESM1(BGC) output, while not perfect, appears adequate to constrain vertical and lateral transport at large scales. The application of a box model assumes that the water in each box is well mixed. For the Arctic Ocean, complex mesoscale hydrodynamics likely degrades the fit with the full model, introducing small biases in box model estimates for salinity, temperature, nitrate, and age. With these limits, the box model is best suited for diagnosing long-term changes in lateral and vertical transport for the Arctic Ocean as a whole.

4.3. Regression Model

A multiple linear regression model for export production (POC flux at 100 m) was created as a function of model surface PAR and mean NO_3 averaged over the 0–100 m depth interval. In the Arctic Ocean, physical factors impose a strong control on plankton productivity, and their impacts are captured in the spatial and temporal patterns of nutrient and light availability. The regression model can be represented as follows:

$$POC\ flux\ (x,\ t) = a + b \times PAR(x,\ t) + c \times NO_3(x,\ t)$$

where x and t indicate the grid cell spatial location and time.

We use the spatial-temporal distribution of monthly estimates from CESM1(BGC) in the year of 1990 to construct the regression model, which produces the coefficients of $a= -0.05$ g C m^{-2} day^{-1}, $b=$ 0.009 g C day^{-1} W^{-1}, and $c=$ 0.006 g C m day^{-1} mmol^{-1}. The space–time structure of monthly export production obtained with the coefficients during the year 1990 was highly correlated with that from the full model (0.81). The main errors in the regression model occur in regions that are affected by horizontal advection: the southern part of the Chukchi sector and Atlantic inflow in the Greenland sector (Figure S6c). Using the regression model derived from CESM1(BGC) state in the year 1990, the regression model can predict reasonably well the change of export production simulated by the CESM1(BGC) (Figure S6d).

Data Availability Statement

The long-term ESM output can be accessed on CMIP5 website (https://esgf-node.llnl.gov/search/cmip5/). The MODIS-Aqua satellite chlorophyll can be accessed online (https://oceandata.sci.gsfc.nasa.gov/MODIS-Aqua/Mapped/Monthly_Climatology/9km/chlor_a/). The ice fraction data can be accessed online (ftp://sidads.colorado.edu/pub/DATASETS/NOAA/G02202_V3/).

Acknowledgments
This research was supported by the Reducing Uncertainties in Biogeochemical Interactions through Synthesis and Computation Scientific Focus Area (RUBISCO SFA), which is sponsored by the Regional and Global Model Analysis (RGMA) Program in the Climate and Environmental Sciences Division (CESD) of Biological and Environmental Research (BER) in the U.S. Department of Energy Office of Science, as well as DOE BER Earth System Modeling Program grant DE-SC0016539 to J. K. M. and F. P. We also thank the reviewers for their constructive comments.

References

Aagaard, K., & Carmack, E. C. (1989). The role of sea ice and other fresh-water in the Arctic circulation. *Journal of Geophysical Research*, *94*(C10), 14,485–14,498. https://doi.org/10.1029/JC094iC10p14485

Ardyna, M., Babin, M., Gosselin, M., Devred, E., Rainville, L., & Tremblay, J. E. (2014). Recent Arctic Ocean sea ice loss triggers novel fall phytoplankton blooms. *Geophysical Research Letters*, *41*, 6207–6212. https://doi.org/10.1002/2014GL061047

Arrigo, K. R., & van Dijken, G. L. (2011). Secular trends in Arctic Ocean net primary production. *Journal of Geophysical Research*, *116*, C09011. https://doi.org/10.1029/2011JC007151

Arrigo, K. R., & van Dijken, G. L. (2015). Continued increases in Arctic Ocean primary production. *Progress in Oceanography*, *136*, 60–70. https://doi.org/10.1016/j.pocean.2015.05.002

Bintanja, R., Katsman, C. A., & Selten, F. M. (2018). Increased Arctic precipitation slows down sea ice melt and surface warming. *Oceanography*, *31*(2), 118–125. https://doi.org/10.5670/oceanog.2018.204

Caesar, J., Palin, E., Liddicoat, S., Lowe, J., Burke, E., Pardaens, A., et al. (2013). Response of the HadGEM2 earth system model to future greenhouse gas emissions pathways to the year 2300. *Journal of Climate*, *26*(10), 3275–3284. https://doi.org/10.1175/JCLI-D-12-00577.1

Carmack, E., & McLaughlin, F. (2011). Towards recognition of physical and geochemical change in subarctic and Arctic seas. *Progress in Oceanography*, *90*(1–4), 90–104. https://doi.org/10.1016/j.pocean.2011.02.007

Carmack, E., Polyakov, I., Padman, L., Fer, I., Hunke, E., Hutchings, J., et al. (2015). Toward quantifying the increasing role of oceanic heat in sea ice loss in the new arctic. *Bulletin of the American Meteorological Society*, *96*(12), 2079–2105. https://doi.org/10.1175/bams-d-13-00177.1

Carmack, E. C., Yamamoto-Kawai, M., Haine, T. W. N., Bacon, S., Bluhm, B. A., Lique, C., et al. (2016). Freshwater and its role in the Arctic marine system: Sources, disposition, storage, export, and physical and biogeochemical consequences in the Arctic and global oceans. *Journal of Geophysical Research: Biogeosciences*, *121*, 675–717. https://doi.org/10.1002/2015JG003140

Ceballos-Romero, E., Le Moigne, F. A. C., Henson, S., Marsay, C. M., Sanders, R., Garcia-Tenorio, R., & Villa-Alfageme, M. (2016). Influence of bloom dynamics on particle export efficiency in the North Atlantic: A comparative study of radioanalytical techniques and sediment traps. *Marine Chemistry*, *186*, 198–210. https://doi.org/10.1016/j.marchem.2016.10.001

Collins, M., Knutti, R., Arblaster, J. M., Dufresne, J.-L., Fichefet, T., Friedlingstein, P., et al. (2013). Long-term climate change: Projections, commitments and irreversibility. In T. F. Stocker et al. (Eds.), *Climate Change 2013: The Physical Science Basis. Contribution of Working Group I to the Fifth Assessment Report of the Intergovernmental Panel on Climate Change* (pp. 1029–1136). Cambridge University Press. https://doi.org/10.1017/CBO9781107415324.024

Coupel, P., Ruiz-Pino, D., Sicre, M. A., Chen, J. F., Lee, S. H., Schiffrine, N., et al. (2015). The impact of freshening on phytoplankton production in the Pacific Arctic Ocean. *Progress in Oceanography*, *131*, 113–125. https://doi.org/10.1016/j.pocean.2014.12.003

Danabasoglu, G., Bates, S. C., Briegleb, B. P., Jayne, S. R., Jochum, M., Large, W. G., et al. (2012). The CCSM4 ocean component. *Journal of Climate*, *25*(5), 1361–1389. https://doi.org/10.1175/JCLI-D-11-00091.1

Dee, D. P., Uppala, S. M., Simmons, A. J., Berrisford, P., Poli, P., Kobayashi, S., et al. (2011). The ERA-Interim reanalysis: Configuration and performance of the data assimilation system. *Quarterly Journal of the Royal Meteorological Society*, *137*(656), 553–597. https://doi.org/10.1002/qj.828

Dong, S. F., Garzoli, S., Baringer, M., Meinen, C., & Goni, G. (2009). Interannual variations in the Atlantic meridional overturning circulation and its relationship with the net northward heat transport in the South Atlantic. *Geophysical Research Letters*, *36*, L20606. https://doi.org/10.1029/2009GL039356

Drijfhout, S. (2015). Competition between global warming and an abrupt collapse of the AMOC in Earth's energy imbalance. *Scientific Reports*, *5*(1), 14877. https://doi.org/10.1038/srep14877

Durack, P. J., Wijffels, S. E., & Matear, R. J. (2012). Ocean salinities reveal strong global water cycle intensification during 1950 to 2000. *Science*, *336*(6080), 455–458. https://doi.org/10.1126/science.1212222

Fu, W. W., Primeau, F., Moore, J. K., Lindsay, K., & Randerson, J. (2018). Reversal of increasing tropical ocean hypoxia trends with sustained climate warming. *Global Biogeochemical Cycles*, *32*, 551–564. https://doi.org/10.1002/2017GB005788

Giorgetta, M. A., Jungclaus, J., Reick, C. H., Legutke, S., Bader, J., Böttinger, M., et al. (2013). Climate and carbon cycle changes from 1850 to 2100 in MPI-ESM simulations for the coupled model intercomparison project phase 5. *Journal of Advances in Modeling Earth Systems*, *5*, 572–597. https://doi.org/10.1002/jame.20038

Haine, T. W. N., Curry, B., Gerdes, R., Hansen, E., Karcher, M., Lee, C., et al. (2015). Arctic freshwater export: Status, mechanisms, and prospects. *Global and Planetary Change*, *125*, 13–35. https://doi.org/10.1016/j.gloplacha.2014.11.013

Hezel, P. J., Fichefet, T., & Massonnet, F. (2014). Modeled Arctic sea ice evolution through 2300 in CMIP5 extended RCPs. *The Cryosphere*, *8*(4), 1195–1204. https://doi.org/10.5194/tc-8-1195-2014

Hopwood, M. J., Carroll, D., Dunse, T., Hodson, A., Holding, J. M., Iriarte, J. L., et al. (2020). Review article: How does glacier discharge affect marine biogeochemistry and primary production in the Arctic? *The Cryosphere*, *14*(4), 1347–1383. https://doi.org/10.5194/tc-14-1347-2020

Hu, A. X., Meehl, G. A., Han, W. Q., Lu, J. H., & Strand, W. G. (2013). Energy balance in a warm world without the ocean conveyor belt and sea ice. *Geophysical Research Letters*, *40*, 6242–6246. https://doi.org/10.1002/2013GL058123

Jahn, A., Aksenov, Y., de Cuevas, B. A., de Steur, L., Häkkinen, S., Hansen, E., et al. (2012). Arctic ocean freshwater: How robust are model simulations? *Journal of Geophysical Research*, *117*, C00D16. https://doi.org/10.1029/2012JC007907

Keigwin, L. D., Klotsko, S., Zhao, N., Reilly, B., Giosan, L., & Driscoll, N. W. (2018). Deglacial floods in the Beaufort Sea preceded Younger Dryas cooling. *Nature Geoscience*, *11*(8), 599–604. https://doi.org/10.1038/s41561-018-0169-6

Kipp, L. E., Charette, M. A., Moore, W. S., Henderson, P. B., & Rigor, I. G. (2018). Increased fluxes of shelf-derived materials to the central Arctic ocean. *Science Advances*, *4*(1), eaao1302. https://doi.org/10.1126/sciadv.aao1302

Koenigk, T., Mikolajewicz, U., Haak, H., & Jungclaus, J. (2007). Arctic freshwater export in the 20th and 21st centuries. *Journal of Geophysical Research*, *112*, G04S41. https://doi.org/10.1029/2006JG000274

Le Fouest, V., Babin, M., & Tremblay, J. E. (2013). The fate of riverine nutrients on Arctic shelves. *Biogeosciences*, *10*(6), 3661–3677. https://doi.org/10.5194/bg-10-3661-2013

Le Moigne, F. A. C., Poulton, A. J., Henson, S. A., Daniels, C. J., Fragoso, G. M., Mitchell, E., et al. (2015). Carbon export efficiency and phytoplankton community composition in the Atlantic sector of the Arctic Ocean. *Journal of Geophysical Research: Oceans*, *120*, 3896–3912. https://doi.org/10.1002/2015JC010700

Li, W. K. W., McLaughlin, F. A., Lovejoy, C., & Carmack, E. C. (2009). Smallest algae thrive as the Arctic Ocean freshens. *Science*, *326*(5952), 539–539. https://doi.org/10.1126/science.1179798

Mahowald, N. M., Randerson, J. T., Lindsay, K., Munoz, E., Doney, S. C., Lawrence, P., et al. (2017). Interactions between land use change and carbon cycle feedbacks. *Global Biogeochemical Cycles*, *31*, 96–113. https://doi.org/10.1002/2016GB005374

McPhee, M. G., Proshutinsky, A., Morison, J. H., Steele, M., & Alkire, M. B. (2009). Rapid change in freshwater content of the Arctic Ocean. *Geophysical Research Letters*, *36*, L10602. https://doi.org/10.1029/2009GL037525

Mioduszewski, J., Vavrus, S., & Wang, M. Y. (2018). Diminishing arctic sea ice promotes stronger surface wind. *Journal of Climate*, *31*(19), 8101–8119. https://doi.org/10.1175/JCLI-D-18-0109.1

Misumi, K., Lindsay, K., Moore, J., Doney, S., Bryan, F., Tsumune, D., & Yoshida, Y. (2014). The iron budget in ocean surface waters in the 20th and 21st centuries: Projections by the community earth system model version 1. *Biogeosciences*, *11*(1), 33–55. https://doi.org/10.5194/bg-11-33-2014

Moore, J. K., Doney, S. C., & Lindsay, K. (2004). Upper ocean ecosystem dynamics and iron cycling in a global three-dimensional model. *Global Biogeochemical Cycles*, *18*, GB4028. https://doi.org/10.1029/2004GB002220

Moore, J. K., Fu, W. W., Primeau, F., Britten, G. L., Lindsay, K., Long, M., et al. (2018). Sustained climate warming drives declining marine biological productivity. *Science*, *359*(6380), 1139–1143. https://doi.org/10.1126/science.aao6379

Moore, J. K., Lindsay, K., Doney, S., Long, M. C., & Misumi, K. (2013). Marine ecosystem dynamics and biogeochemical cycling in the community earth system model [CESM1(BGC)]: Comparison of the 1990s with the 2090s under the RCP4.5 and RCP8.5 scenarios. *Journal of Climate*, *26*(23), 9291–9312. https://doi.org/10.1175/JCLI-D-12-00566.1

Nummelin, A., Ilicak, M., Li, C., & Smedsrud, L. H. (2016). Consequences of future increased Arctic runoff on Arctic Ocean stratification, circulation, and sea ice cover. *Journal of Geophysical Research: Oceans*, *121*, 617–637. https://doi.org/10.1002/2015JC011156

Oldenburg, D., Armour, K. C., Thompson, L., & Bitz, C. M. (2018). Distinct mechanisms of ocean heat transport into the arctic under internal variability and climate change. *Geophysical Research Letters*, *45*, 7692–7700. https://doi.org/10.1029/2018GL078719

Pemberton, P., & Nilsson, J. (2016). The response of the central Arctic Ocean stratification to freshwater perturbations. *Journal of Geophysical Research: Oceans*, *121*, 792–817. https://doi.org/10.1002/2015JC011003

Peng, G., Meier, W. N., Scott, D. J., & Savoie, M. H. (2013). A long-term and reproducible passive microwave sea ice concentration data record for climate studies and monitoring. *Earth System Science Data*, *5*(2), 311–318. https://doi.org/10.5194/essd-5-311-2013

Peterson, B. J., Holmes, R. M., McClelland, J. W., Vorosmarty, C. J., Lammers, R. B., Shiklomanov, A. I., et al. (2002). Increasing river discharge to the Arctic Ocean. *Science*, *298*(5601), 2171–2173. https://doi.org/10.1126/science.1077445

Polyakov, I. V., Pnyushkov, A. V., Rember, R., Padman, L., Carmack, E. C., & Jackson, J. M. (2013). Winter convection transports Atlantic water heat to the surface layer in the eastern Arctic Ocean. *Journal of Physical Oceanography*, *43*(10), 2142–2155. https://doi.org/10.1175/jpo-d-12-0169.1

Popova, E. E., Yool, A., Coward, A. C., Dupont, F., Deal, C., Elliott, S., et al. (2012). What controls primary production in the Arctic Ocean? Results from an intercomparison of five general circulation models with biogeochemistry. *Journal of Geophysical Research*, *117*, C00D12. https://doi.org/10.1029/2011JC007112

Randelhoff, A., Holding, J., Janout, M., Sejr, M. K., Babin, M., Tremblayu, J. E., & Alkire, M. B. (2020). Pan-Arctic ocean primary production constrained by turbulent nitrate fluxes. *Frontiers in Marine Science*, *7*, 150. https://doi.org/10.3389/fmars.2020.00150

Randerson, J. T., Lindsay, K., Munoz, E., Fu, W., Moore, J. K., Hoffman, F. M., et al. (2015). Multicentury changes in ocean and land contributions to the climate-carbon feedback. *Global Biogeochemical Cycles*, *29*, 744–759. https://doi.org/10.1002/2014GB005079

Rennermalm, A. K., Wood, E. F., Dery, S. J., Weaver, A. J., & Eby, M. (2006). Sensitivity of the thermohaline circulation to Arctic Ocean runoff. *Geophysical Research Letters*, *33*, L12703. https://doi.org/10.1029/2006GL026124

Reyes, F. R., & Lougheed, V. L. (2015). Rapid nutrient release from permafrost thaw in arctic aquatic ecosystems. *Arctic Antarctic and Alpine Research*, *47*(1), 35–48. https://doi.org/10.1657/Aaar0013-099

Shu, Q., Qiao, F. L., Song, Z. Y., Zhao, J. C., & Li, X. F. (2018). Projected freshening of the Arctic Ocean in the 21st century. *Journal of Geophysical Research: Oceans*, *123*, 9232–9244. https://doi.org/10.1029/2018JC014036

Slagstad, D., Wassmann, P. F. J., & Ellingson, I. (2015). Physical constrains and productivity in the future Arctic Ocean. *Frontiers in Marine Science*, *2*. https://doi.org/10.3389/fmars.2015.00085

Tank, S. E., Manizza, M., Holmes, R. M., McClelland, J. W., & Peterson, B. J. (2012). The processing and impact of dissolved riverine nitrogen in the Arctic Ocean. *Estuaries and Coasts*, *35*(2), 401–415. https://doi.org/10.1007/s12237-011-9417-3

Tedesco, L., Vichi, M., & Scoccimarro, E. (2019). Sea-ice algal phenology in a warmer Arctic. *Science Advances*, *5*(5), eaav4830. https://doi.org/10.1126/sciadv.aav4830

Torres-Valdés, S., Tsubouchi, T., Bacon, S., Naveira-Garabato, A. C., Sanders, R., McLaughlin, F. A., et al. (2013). Export of nutrients from the Arctic Ocean. *Journal of Geophysical Research: Oceans*, *118*, 1625–1644. https://doi.org/10.1002/jgrc.20063

Tremblay, J.-E., Anderson, L. G., Matrai, P., Coupel, P., Belanger, S., Michel, C., & Reigstad, M. (2015). Global and regional drivers of nutrient supply, primary production and CO_2 drawdown in the changing Arctic Ocean. *Progress in Oceanography*, *139*, 171–196. https://doi.org/10.1016/j.pocean.2015.08.009

Vancoppenolle, M., Bopp, L., Madec, G., Dunne, J., Ilyina, T., Halloran, P. R., & Steiner, N. (2013). Future Arctic Ocean primary productivity from CMIP5 simulations: Uncertain outcome, but consistent mechanisms. *Global Biogeochemical Cycles*, *27*, 605–619. https://doi.org/10.1002/gbc.20055

van Vuuren, D. P., Edmonds, J., Kainuma, M., Riahi, K., Thomson, A., Hibbard, K., et al. (2011). The representative concentration pathways: An overview. *Climatic Change*, *109*(1–2), 5–31. https://doi.org/10.1007/s10584-011-0148-z

Veraverbeke, S., Rogers, B. M., Goulden, M. L., Jandt, R. R., Miller, C. E., Wiggins, E. B., & Randerson, J. T. (2017). Lightning as a major driver of recent large fire years in North American boreal forests. *Nature Climate Change*, *7*(7), 529–534. https://doi.org/10.1038/Nclimate3329

Williams, W. J., & Carmack, E. C. (2015). The 'interior' shelves of the Arctic Ocean: Physical oceanographic setting, climatology and effects of sea-ice retreat on cross-shelf exchange. *Progress in Oceanography*, *139*, 24–41. https://doi.org/10.1016/j.pocean.2015.07.008

Yang, H. J., Wang, K., Dai, H. J., Wang, Y. X., & Li, Q. (2016). Wind effect on the Atlantic meridional overturning circulation via sea ice and vertical diffusion. *Climate Dynamics*, *46*(11–12), 3387–3403. https://doi.org/10.1007/s00382-015-2774-z

Yang, Q., Dixon, T. H., Myers, P. G., Bonin, J., Chambers, D., van den Broeke, M. R., et al. (2016). Recent increases in Arctic freshwater flux affects Labrador Sea convection and Atlantic overturning circulation. *Nature Communications*, *7*(1), 10525. https://doi.org/10.1038/ncomms10525